A complex of iron and nucleic acid catabolites is a signal that triggers differentiation in a freshwater protozoan

Harriett E. Smith-Somerville*†‡, John K. Hardman*, Russell Timkovich†§, William J. Ray*¶, Karen E. Rose*, Phillip E. Ryals‖, Sandra H. Gibbons††, and Howard E. Buhse, Jr.****

*Section in Molecular and Cellular Biology, Department of Biological Sciences, §Department of Chemistry and †Coalition for Biomolecular Products, University of Alabama, Tuscaloosa, AL 35487; ‖Department of Biochemistry and Molecular Biology, Mississippi State University, Mississippi State, MS 39762; and **Department of Biological Sciences, University of Illinois, Chicago, IL 60607-0607

Edited by David M. Prescott, University of Colorado, Boulder, CO, and approved May 3, 2000 (received for review October 22, 1999)

The polymorphic ciliated protozoan *Tetrahymena vorax* can undergo differentiation from the microstomal form, which normally feeds on bacteria and other particulate matter, into the macrostomal cell type, which is capable of ingesting prey ciliates. The process is triggered by exposure of the microstome to an inducer contained in stomatin, an exudate of the prey. To establish the identity of the signal, stomatin was fractionated by combinations of cation exchange, HPLC, and TLC, and the fractions were assayed for biological activity. Although no single active fraction of purified inducer was obtained, all fractions with activity contained ferrous iron and the nucleic acid catabolites hypoxanthine (6-oxypurine) and uracil (2,4-dioxopyrimidine), probably in a chelated form. The activity of synthetic complexes containing these three components is equivalent to stomatin. These results indicate a role for ferrous iron and its potential in chelated form to signal differentiation in certain protozoa and, perhaps, in other organisms as well.

Iron is an essential trace metal for virtually all organisms as a component of oxygen transport proteins and antioxidants, and as a cofactor for a variety of enzymes including oxidases and ribonucleotide reductases. The low solubility of iron oxide, the usual state of the unbound metal in an aerobic environment, has required the development of specialized transport mechanisms, and most known bioactive extracellular iron complexes are involved in this process (1–3). For uptake into mammalian cells, iron usually is bound to transferrin, although transferrin-independent transport through a ferrous iron carrier has been reported (4–7). Most prokaryotic cells and certain fungi, algae, and plants secrete siderophores that chelate ferric iron for uptake via specific transport systems. Here we report a role for an extracellular iron-nucleic acid catabolite complex as a trigger for differentiation in the freshwater, polymorphic ciliate, *Tetrahymena vorax*.

During starvation stress, *T. vorax* can undergo extensive cellular remodeling to use an alternative source of food. This protozoan normally exists in the microstomal (''small-mouth'') cell type that concentrates suspended particles in phagosomes formed sequentially at the base of the oral apparatus (Fig. 1). When removed from nutrient medium and supplied with an external stimulus, the cell transforms into the macrostomal cell type that is capable of ingesting prey ciliates. This cell type differs from the microstomal form in size and organization of the oral apparatus and development of the cytopharyngeal pouch, a nascent vacuole large enough to accommodate the prey (8–10).

Previous studies have shown that differentiation is initiated by a factor present in a crude water-soluble exudate termed stomatin by Buhse (11) who first isolated it from a prey protozoan, *T. pyriformis.* [Ciliate stomatin, named by Buhse (11) in 1967, should not be confused with the protein from the red cell membrane given the same name by Stewart *et al.* (38) in 1993.] Active crude exudate has been derived from two additional species of *Tetrahymena* (*T. thermophila* and *T. membris*) and from *Paramecium tetraurelia* (refs. 12 and 13; P.E.R., unpublished observations). Stomatin appears pale yellow and has several absorbance peaks including a broad peak with an absorbance maximum near 254 nm. The crude material contains numerous components including sugars and amino acids, small amounts of phospholipids, tetrahymanol, and free fatty acids (14). Nucleic acid catabolites, particularly hypoxanthine and either uridine (12) or uracil (15), the end products of purine and pyrimidine catabolism in *Tetrahymena*, are also present. The active factor in stomatin is heat and cold stable (11, 12), has a molecular mass below 1,800 Da based on Biogel P2 chromatography (12), and is contained only in fractions with high absorbance at 260 nm (12). The active factor is most effective at an acidic pH (16). Hypoxanthine augmented by uridine was reported to generate large percentages of macrostomal cells in populations of *T. vorax* (12). These results could not be duplicated in other laboratories (11, 13), but suggested that these components might participate in some manner in differentiation.

Materials and Methods

Reagents. BSA, alanine, hypoxanthine, uracil, inosine, 3′-IMP, 5′-IMP, cIMP, inosine 5′-diphosphate (IDP), IDP-ribose, and 2,2-bipyridyl were purchased from Sigma. Ferrous sulfate ($FeSO_4 \cdot 7H_2O$) was obtained from Curtain Matheson Scientific, Houston, and Sigma.

Preparation of Stomatin. Liter cultures of *T. pyriformis* GL grown in enriched proteose peptone medium (17, 18) were concentrated by centrifugation, washed, and suspended in distilled, deionized H_2O at 0.1 vol of the original culture, and incubated overnight at 20°C in two Roux flasks. The suspension was centrifuged repeatedly to remove the cells; the supernatant was filtered through a 0.45-μm filter, dried by rotary evaporation, dissolved in distilled, deionized H_2O at a final concentration of 60 mg/ml, and stored at −80°C.

Chromatography. Cation-exchange chromatography of stomatin was performed on a 1 × 54-cm column containing Dowex-50 resin (H^+ form, 4%, 200–400 mesh) equilibrated in 3 mM

This paper was submitted directly (Track II) to the PNAS office.

Abbreviation: IDP, inosine 5′-diphosphate.

‡To whom reprint requests should be addressed at: Department of Biological Sciences, University of Alabama, Box 870344, Tuscaloosa, AL 35487-0344. E-mail: hsmithso@ua.edu.

¶Present address: Department of Psychiatry, Washington University School of Medicine, St. Louis, MO 63110.

††Present address: Moraine Valley Community College, Palos Hills, IL 60465.

The publication costs of this article were defrayed in part by page charge payment. This article must therefore be hereby marked "*advertisement*" in accordance with 18 U.S.C. §1734 solely to indicate this fact.

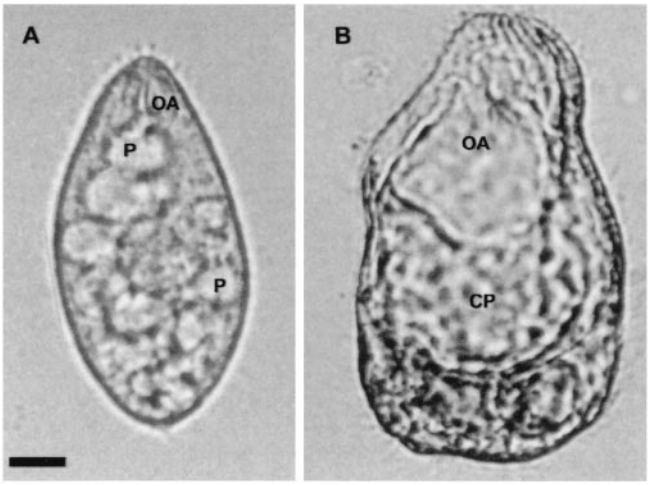

Fig. 1. Cell types of *T. vorax*. (*A*) Microstomal cell type. (*B*) Macrostomal cell type. Differentiation involves the replacement of the small oral apparatus (OA) in the microstomal form with the large oral apparatus characteristic of the macrostomal cell type and development of the cytopharyngeal pouch (CP) in the place of small phagosomes (P). (Bar represents 10 μm.)

KH_2PO_4, pH 4.9. Stomatin (60 mg, approximately 300 A_{254} units) in distilled, deionized H_2O was placed on the column and eluted in a linear pH gradient formed by using 150 ml each of 3 mM KH_2PO_4 and 3 mM K_2HPO_4, at a flow rate of 0.72 ml/min. Fractions were monitored by absorbance at 254 nm, and fractions collected from peaks were pooled. At the end of the gradient, the column was further eluted with additional K_2HPO_4, followed by 3.7 M NH_4OH. With the exception of those eluted with NH_4OH, combined fractions were adjusted to pH 6.8 with 0.1 M HCl or 0.1 M NaOH, dried by rotary evaporation and dissolved in distilled, deionized H_2O to a concentration of 10 A_{254} units/ml. Fractions eluted with NH_4OH were combined, dried, and dissolved in 3 mM potassium phosphate buffer, pH 6.8, to a concentration of 10 A_{254} units/ml. Fractions were stored at -80°C.

Reversed-phase HPLC was performed by using a C_{18} μBondapak column (Waters, 3.9 $\times$ 300 mm) and a mobile phase of one of the following: (*i*) HPLC-grade H_2O, (*ii*) 2% (vol/vol) acetic acid/10% (vol/vol) methanol, (*iii*) 50 mM ammonium dihydrogen phosphate adjusted to pH 6 with concentrated NH_4OH (19), (*iv*) a linear concentration gradient of acetonitrile (0–100%) at flow rates indicated in figure legends, or (*v*) 50 mM citrate buffer, pH 5. The eluate was monitored at wavelengths indicated in the figures. Fractions exhibiting absorbance were dried by rotary evaporation, dissolved in a volume of HPLC-grade H_2O equal to the initial injection volume, and stored at -80°C.

TLC of stomatin and selected HPLC fractions was performed on Whatman K6F silica gel plates with fluorescent indicator by using NH_4OH/isopropanol/distilled, deionized H_2O (7:1.5:1.5, by vol) as the mobile phase. Hypoxanthine, uracil, inosine, 3′-IMP, 5′-IMP, cIMP, IDP, and IDP-ribose were used as standards. To obtain a sufficient quantity for HPLC analysis and bioactivity assays, preparative TLC was performed on selected fractions. The band of interest was scraped from the dried plate, eluted in HPLC-grade H_2O, dried by rotary evaporation, and dissolved in a volume of HPLC-grade H_2O equal to the volume of the fraction initially loaded onto the preparative plate. The eluted fractions were stored at -80°C.

Assay for Biological Activity. *T. vorax* V_2S was grown axenically at 20°C in 50 ml of either enriched proteose peptone medium or Loefer's medium (20). Cell density was determined by using a Coulter Counter model ZBI. Populations in late logarithmic phase of growth were concentrated by centrifugation, washed in inorganic medium (21), pH 6.8, and suspended in inorganic medium to give a cell density of 4×10^4 cells contained in a final volume of 100 μl. Stomatin (3 mg/ml final concentration), a stomatin fraction, or one of the synthetic inducers was added, and the cells were incubated at 20°C for 7 h. An equal volume of distilled, deionized H_2O was used in place of the test solution as a routine control, and the particular mobile phase prepared in the same manner as the fraction was included as an additional control when appropriate. Activity was determined microscopically by counting the number of macrostomal cells in a minimum of 500 total cells.

Protein Determination. Protein concentration was determined by the bicinchoninic acid method (22) and the Bio-Rad Protein Assay based on the method of Bradford (23) using BSA and alanine as standards.

Iron Determination. Stock solutions (10 mM and 50 mM) were prepared by dissolving 2,2-bipyridyl in either DMSO or 95% ethanol. Aliquots of stomatin or fractions were tested for the presence of the rose color diagnostic for ferrous iron in a solution containing a final concentration of 0.5–3 mM 2,2-bipyridyl with and without ascorbate (100–133 μM final concentration). A Beckman Synchron CX7 Delta automated clinical analyzer was used for quantitative determinations of total iron.

Spectroscopic Methods. Absorbance spectra of stomatin and stomatin fractions were obtained by using a Perkin–Elmer Lambda 3A UV/VIS recording spectrophotometer. Absorption maxima were determined by scanning the sample at wavelengths between either 600 or 450 nm and 190 nm. A Bruker AM 500 spectrometer operating at 500 MHz was used to record all proton NMR spectra.

Preparation of Iron Chelates (Synthetic Inducer). Chelates were prepared by three different procedures. One preparation was based on the method of Albert (24) except that uracil was added to the solution. For this method, a solution containing 0.33 mM hypoxanthine, 0.7 mM uracil, and 3.3 mM $FeSO_4 \cdot 7H_2O$ in HPLC-grade H_2O was heated at 37°C for 15 min. To test for biological activity, peaks collected from multiple preparative HPLC separations (250 μl/injection) were combined, dried by rotary evaporation, and dissolved in HPLC-grade H_2O. In the second procedure, hypoxanthine (1 mM), uracil (1 mM), and $FeSO_4 \cdot 7H_2O$ (2 mM) were dissolved in HPLC-grade H_2O acidified with reagent-grade concentrated H_2SO_4 to approximately pH 2.4 to maintain iron in the ferrous form. This solution was stored overnight at 4°C, and the pH was adjusted to 5 with KOH as described by Nelsen *et al.* (17). For the third complex, $FeSO_4$ was substituted for $CuSO_4$ and uracil was added in the procedure of Acevedo-Chávez *et al.* (25). Briefly, a solution containing 10 mM hypoxanthine, 10 mM uracil, 20 mM $FeSO_4 \cdot 7H_2O$, 2.5 mM glycine, 2.5 mM NaCl, and 50 mM HCl was stirred for 2 weeks at room temperature and dried at 50°C for 2 days. The surface of the dried residue was washed gently with ice-cold HPLC-grade H_2O. The washed residue was dried at 50°C and stored at 4°C. Before use, the chelate was dissolved in HPLC-grade H_2O and adjusted to pH 5 with KOH, or in 50 mM citrate buffer, pH 5.

Results and Discussion

Separation and Properties of Active Fractions from Stomatin. Initial attempts to separate the active component of stomatin by using different types of column chromatography failed to yield a unique active fraction. The active component(s) binds to Dowex-50 cation-exchange resin, indicating that it is cationic, but

does not elute as a discrete fraction. Treatment of *T. vorax* with aliquots from either of two Dowex-50 fractions eluting at a pH in the range of 5.5 to 6 consistently yielded a higher percentage of differentiated cells than other collected fractions. Both fractions had absorbance maxima at 247 and 270 nm; however, these peaks were broad so that the 270-nm absorbance peak was a shoulder on the 247-nm peak. The 247-nm absorption peak declined from the maximum to about 235 nm, followed by a sharp increase in absorbance to the end of the spectral scan at 190 nm. When subjected to reversed-phase HPLC using ammonium dihydrogen phosphate as the mobile phase, both fractions separated into additional peaks, but the activity was confined to a group of small peaks that eluted with or immediately after the void volume of the column. We were unable to find conditions that would permit separation of these peaks on a reversed-phase column. Reversed-phase HPLC of crude stomatin yielded active fractions having identical retention times to the active fractions from HPLC chromatography of the active Dowex-50 fractions. This revealed that these peaks could be separated directly from stomatin without initial cation-exchange chromatography simplifying the enrichment protocol.

The active fractions from stomatin obtained by reversed-phase HPLC using H_2O, ammonium dihydrogen phosphate, or an acetonitrile gradient are shown in Fig. 2 *A*, *B*, and *D*. Authentic, commercially obtained uracil comigrated with one of two major absorbance peaks in stomatin, and authentic hypoxanthine coeluted with the other major peak. Active fractions eluted just after the void volume (Fig. 2*A*, fraction 1), and at a retention time of 43 min (Fig. 2A, fraction 3) at a flow rate of 1 ml/min when the mobile phase was H_2O or ammonium dihydrogen phosphate. With the acetonitrile gradient, the most active fractions eluted just after the void volume and at 100% acetonitrile (Fig. 2*B*, fraction 4). The elution profile of the initial fraction obtained by using H_2O as the mobile phase mirrored that of stomatin when rechromatographed by using the acetonitrile gradient (data not shown).

When we compared the migration patterns of stomatin and the active HPLC fractions (shown in Fig. 2) by TLC, each contained a major spot that comigrated with hypoxanthine and uracil standards and triggered differentiation when recovered from the TLC plate (Fig. 3, arrow). Other hypoxanthine derivatives (inosine, 3′-IMP, 5′-IMP, cIMP, IDP and IDP-ribose) did not comigrate with this major spot and did not induce differentiation; thus, these were eliminated from consideration. Each fraction also exhibited one or more spots with lesser mobilities upon TLC separation (Fig. 3, lanes 2–6), including the recovered TLC fraction itself when rechromatographed (Fig. 3, lane 7), indicating that some of these spots originated from dissociation or degradation of the active component. One peak shared by all of these had as much as 50% of the activity of the major spot (Fig. 3, arrowhead). The peak eluting at 100% acetonitrile contained the fewest spots using TLC compared with the other peaks with activity (Fig. 3, lanes 5 and 6). This fraction gave a positive reading for protein with the bicinchoninic acid method that is based on the formation of a copper-peptide chelate, but not with the Bio-Rad protein assay that measures a color change in an acidic solution of Coomassie brilliant blue G. The Bio-Rad protein assay gave positive readings when we tested solutions containing 1 μg/ml alanine as well as BSA. Thus, because of the lack of a reading for the stomatin fraction using this assay, we concluded that neither peptides nor amino acids were present in detectable amounts.

The HPLC-elution profile (Fig. 2*C*) of the common TLC spot showed three major absorbance peaks, one corresponding to an absorbance peak in the initial void-volume fraction of stomatin and two that comigrated with authentic, commercially obtained uracil and hypoxanthine. The identities of the latter two fractions as uracil and hypoxanthine were confirmed by NMR based on

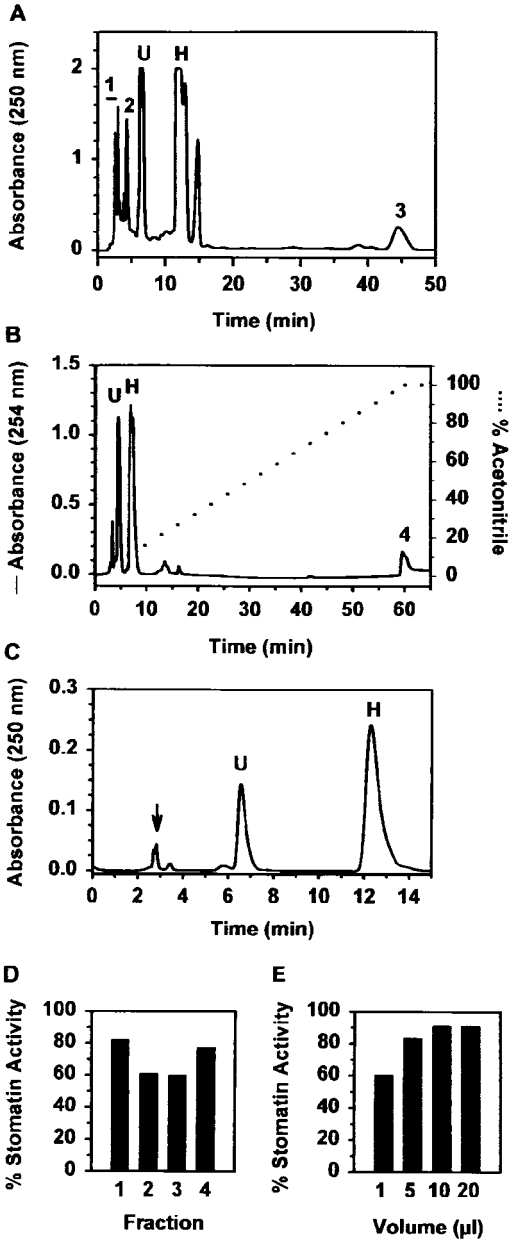

Fig. 2. HPLC elution profiles and activity of stomatin and stomatin fractions obtained by reversed-phase HPLC. (*A*) Elution profile of stomatin using H_2O as the mobile phase at a flow rate of 1 ml/min. A total of 0.6 mg of stomatin (10 μl total volume, 0.138 A_{250} units/μl) was injected. U and H indicate eluting positions of the uracil and hypoxanthine standards, respectively. Equivalent results were obtained with ammonium dihydrogen phosphate as the mobile phase. (*B*) Elution profile of stomatin (straight line) using an acetonitrile gradient (dotted line) as the mobile phase at a flow rate of 1 ml/min. A total of 0.6 mg of stomatin (10 μl total volume, 0.118 A_{254} units/μl) was injected. (*C*) HPLC elution profile of the major spot from fraction 1 in *A* eluted from a TLC plate (Fig. 3, arrow). The injection volume was 10 μl (0.183 A_{250} units/μl). The mobile phase was H_2O at a flow rate of 1 ml/min. Peaks identified as uracil and hypoxanthine by NMR are labeled U and H, respectively. The initial fraction (arrow) consisting of one major plus several small peaks did not generate a NMR signal. (*D*) Maximum activity of fractions 1–3 in *A* and fraction 4 in *B* expressed as a percentage of the activity of stomatin. Fraction 1, 5 μl, 0.363 A_{250} units/μl; fraction 2, 5 μl, 0.112 A_{250} units/μl; fraction 3, 10 μl, 0.097 A_{250} units/μl; fraction 4, 10 μl, 0.042 A_{250} units/μl. Controls contained only H_2O or acetonitrile prepared concurrently with fraction 4. (*E*) Activity of different volumes of the initial fraction in *B* (0.183 A_{250} units/μl) expressed as % of the stomatin activity obtained using the same test population.

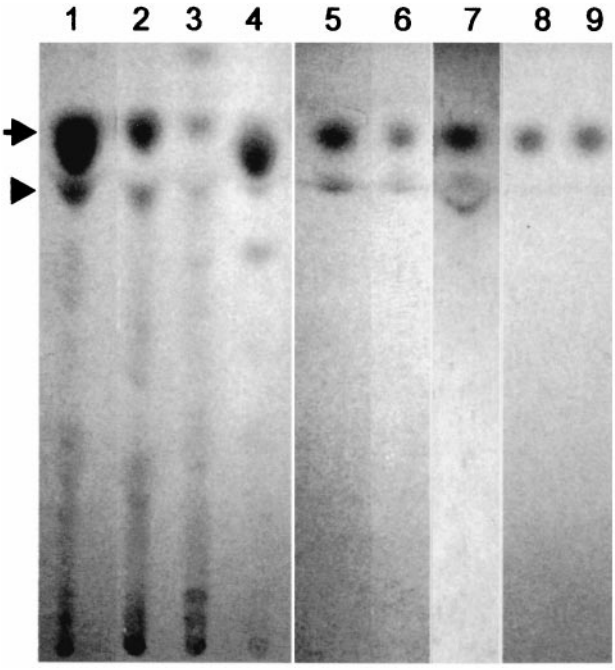

Fig. 3. Thin-layer chromatograms of stomatin and active stomatin fractions. Lane 1, crude stomatin (2 μl, 6 μg); lane 2, peak 1 (shown in Fig. 2*A*, 10 μl) obtained by HPLC separation of stomatin with H_2O as the mobile phase; lane 3, peak 2 (shown in Fig. 2*A*, 20 μl) obtained by HPLC separation of stomatin with H_2O as the mobile phase; lane 4, peak 3 (shown in Fig. 2*A*, 30 μl) obtained by HPLC separation of stomatin with H_2O as the mobile phase; lane 5, peak 4 from stomatin (shown in Fig. 2*B*, 10 μl) eluting at 100% acetonitrile; lane 6, peak eluting at 100% acetonitrile (10 μl) when the initial void-volume fraction was rechromatographed by using the acetonitrile gradient as the mobile phase; lane 7, eluted spot (5 μl) from TLC-purified peak 1 (Fig. 2*A*); lanes 8 and 9, commercially obtained hypoxanthine and uracil standards (25 nmol each) dissolved in H_2O. The major active spot is indicated by the arrow. A spot with lesser activity probably originating from dissociation of the major active component is indicated by the arrowhead.

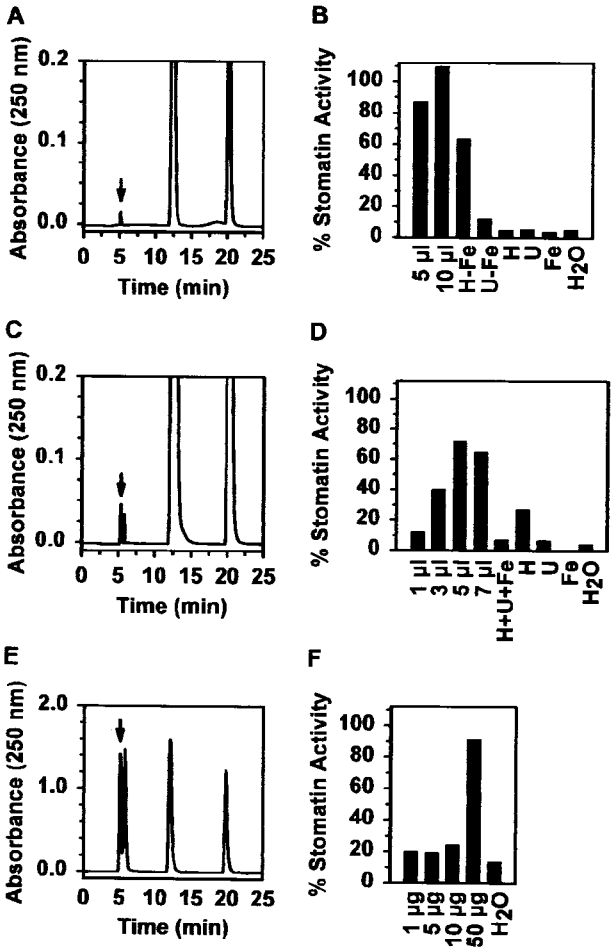

Fig. 4. HPLC elution profiles and activity of solutions containing iron, hypoxanthine, and uracil. Preparations of hypoxanthine/uracil/Fe^{2+} complexes were subjected to HPLC. Each preparation contains peaks corresponding to the active initial void-volume fraction in natural stomatin preparations (arrows) and peaks comigrating with free hypoxanthine and uracil. Activity of test solutions is expressed as % activity of stomatin (3 mg/ml). (*A*) Elution profile of solution (50 μl) containing hypoxanthine, uracil, and $FeSO_4$ prepared based on the procedure described by Albert (24). The mobile phase was H_2O at a flow rate of 0.5 ml/min. (*B*) Activity of the initial void-volume fraction indicated by the arrow in *A* (0.17 A_{250} units/μl) compared with the activity of a fraction prepared in identical manner but using a solution from which uracil was omitted (H-Fe, 5 μl, 0.13 A_{250} units/μl) and a fraction from which hypoxanthine was omitted (U-Fe, 5 μl, 0.26 A_{250} units/μl). The same results were obtained when 10 μl were added. Hypoxanthine (50 μM), uracil (50 μM), $FeSO_4$ (100 μM), and H_2O were substituted for stomatin as controls. (*C*) Elution profile of solution prepared by a procedure modified from Nelsen *et al.* (17). The injection volume was 50 μl and the mobile phase was H_2O at a flow rate of 0.5 ml/min. (*D*) Activity of different concentrations of the unfractionated iron-base solution in *C* compared with the activity of hypoxanthine (50 μM), uracil (50 μM), and $FeSO_4$ (100 μM), tested separately (H, U, Fe) and in combination (H + U + Fe). The activity of solutions made by this method varied, but differentiation as high as 96% of the stomatin control has been obtained. (*E*) Elution profile of solution containing 2 μg of the complex prepared by modification of the procedure described by Acevedo-Chávez *et al.* (25). The mobile phase was 50 mM citrate buffer at a flow rate of 0.5 ml/min. (*F*) Activity of different final concentrations of the unfractionated complex prepared by the method of Acevedo-Chávez *et al.* (25) and dissolved in H_2O and adjusted to pH 5 with KOH.

characteristic resonances in the aromatic region of the spectrum. Initial identification, made on the basis of the chemical shifts, was verified by the observation that the target resonances retained their peak shape but grew in intensity proportional to the amount added when the fractions were spiked with samples of authentic hypoxanthine and uracil (data not shown). When these three HPLC absorbance peaks were collected and assayed for stomatin activity, again only the initial void-volume fraction was active, and the activity was concentration-dependent (Fig. 2*E*). Upon repeated freeze-thawing, the relative size of the initial void-volume peak decreased with a corresponding increase in the size of absorbance peaks for hypoxanthine and uracil. The decrease in the void-volume peak also was associated with a decline in activity. This fraction (Fig. 2*C*, arrow) did not generate a NMR spectrum, suggesting the possibility that paramagnetic metals were present.

Upon addition of 2,2-bipyridyl, stomatin and active fractions obtained by HPLC or TLC separation exhibited the rose color that is diagnostic for Fe^{2+}. No iron was detected in the uracil and hypoxanthine peaks. The presence of iron was confirmed in crude stomatin, several active peaks eluted from HPLC, and the active band recovered from TLC using the Beckman CX7 system. The calculated molar concentration of total iron in these samples ranged from 161 μM in the crude material to 1.18 μM in the fraction eluted from TLC plates. Stomatin loses activity on prolonged storage. Older preparations of stomatin and stomatin fractions that had been stored for 3 or more years gave a faint or negative color reaction with 2,2-bipyridyl, but the distinctive rose color appeared in these preparations after ascorbate was added to reduce Fe^{3+} to Fe^{2+}. Induction of differentiation in the

Table 1. Comparison of the stomatin signal with other released morphogens involved in predator/prey interactions in aquatic environments

	Source of signal					
Property	*Tetrahymena* (ciliate) Stomatin signal	*Chaoborus* (midge) Kairomone	*Asplanchna* (rotifer) signal	*Lembadion* (ciliate) signal	*Amoeba* (ciliate) signal	*Stenostomum* (turbellarian) signal
Appearance	Pale yellow to brownish	Pale yellow to brownish	—	—	—	—
Molecular mass	<1.8 kDa	<0.5 kDa	—	31.5 kDa	5–10 kDa	17.5 kDa
Heat stable (>90°C)	Yes	Yes	No	No	—	No
Stable at low pH	Yes	Yes	—	—	—	—
Protease sensitive	No	No	Yes	Yes	Yes	Yes
Resin binding						
Cationic	Yes	Weak	—	—	—	—
Anionic	No	Yes	—	—	—	—
Released by	Prey	Predator	Predator	Predator	Predator	Predator
Target organism	Polymorphic *Tetrahymena*	*Daphnia* (cladoceran)	*Brachionus* (rotifer)	*Euplotes* (ciliate)	*Euplotes*	*Euplotes*
Molecular form(s)	Multiple	Water: single Homogenate: multiple	Single	Single	Single	Single
Characterized as	Complexed hypoxanthine, uracil and Fe^{2+}	Nonolefinic hydroxyl-carboxylic acid	Protein	Polypeptide	Peptide	Polypeptide
Reference	(11, 12); this paper	(36, 37)	(32)	(29)	(30)	(31)

presence of ascorbate has been noted to enhance macrostome formation (26).

Taken together, these results indicate that (*i*) the active component(s) of stomatin is cationic because it is bound by Dowex-50 and elutes from a reversed-phase C_{18} column at or near the void volume with a variety of mobile phases; (*ii*) it exists in multiple, possibly aggregated forms based on elution of activity over a wide pH range on a Dowex-50 column and in multiple fractions on a reversed-phase C_{18} column including fractions eluting at both the void volume and 100% acetonitrile; and (*iii*) the active fractions eluting at the void volume always contain free hypoxanthine and uracil after being subjected to the disruptive conditions inherent in freeze thawing. The active factor does not consist solely of hypoxanthine and uracil (or uridine as suggested by Butzel and Fisher, ref. 12), but also contains Fe^{2+}. This conclusion is based on the diagnostic color reaction of Fe^{2+} with 2,2-bipyridyl in all active fractions, data from NMR, measurements using the Beckman Synchron CX7 Delta automated clinical analyzer, and the observation that the inducer is most active at acidic pH. The presence of a component that produces a color reaction with bicinchoninic acid but not with Coomassie blue and that interferes with NMR supports the conclusion that a metal in nonpeptide, chelated form is present in active stomatin. Thus, it appeared to us that the active biological component in stomatin consists of a relatively weak complex of ferrous iron, hypoxanthine, and uracil. To test this hypothesis, we synthesized preparations of hypoxanthine/uracil/Fe^{2+} chelates.

Activity of Synthetic Chelates. Chelated Fe^{2+} complexes were synthesized by using modifications of three different procedures. Each of these preparations exhibited peaks in the position of the biologically active void-volume HPLC peaks from stomatin and TLC-purified material (Fig. 4, arrows). Each synthetic complex also induced differentiation in populations of *T. vorax* comparable to native stomatin (Fig. 4). The activity of a complex prepared with hypoxanthine and Fe^{2+}, but omitting uracil, had substantial but reduced activity (Fig. 4*B*). When hypoxanthine was omitted or when equivalent amounts of the three components were added as separate solutions directly to cell suspensions (Fig. 4*D*), the percentage of macrostomes in the test population was comparable to that of the H_2O negative control. The actual percentage of differentiation obtained varies with a given preparation of solution and population; however, similar results have been generated in three different laboratories by using cultures of *T. vorax* grown in either enriched proteose peptone medium containing chelated iron or Loefer's medium, which has no added iron.

A chelated complex of hypoxanthine, uracil, and ferrous iron appears to be the most likely bioactive form. The exact structure with regard to the stoichiometry of the three components has not yet been determined, but current efforts are directed toward elucidation of the structure. Both hypoxanthine and uracil have potential N and O binding sites for metal influenced by several factors including basicity of the site and pH of the environment. Fe^{2+} favors mixed O and N donors (27). Acevedo-Chávez *et al.* (25) reported that copper sulfate and hypoxanthine formed complexes consisting of two Cu^{2+} ions bridged by four hypoxanthine molecules and two SO_4^{2}-ions based on EPR spectral data.

The chelate may interact with a cell-surface receptor and initiate a transmembrane signaling cascade. Ryals *et al.* (28) have presented evidence that treatment of *T. vorax* with several proteases results in a concentration-dependent reduction in differentiation, suggesting that the inducer acts through binding to a surface-exposed protein. They also noted an increase in intracellular polyphosphoinositol concentration with a corresponding decrease in the relative amounts of phosphatidylinositol 4,5-bisphosphate and phosphatidylinositol 1,4,5-trisphosphate within 5 min after exposure to stomatin. The effects of inhibitors implicate the involvement of several signaling cascade components in triggering differentiation.

We have shown that a complex containing iron initiates cellular differentiation. Changes in morphology and/or behavior of prey in response to factors released by predators appear to be widespread, but only in a few cases have the inducers been identified. Characteristics of several released morphogens are compared with the complex obtained from stomatin in Table 1. Ciliates in the genus *Euplotes* display defensive changes in cellular architecture in response to factors released by predators, including the ciliate *Lembadion bullinum* (29), the rhizopod *Amoeba proteus* (30), and the turbellarian *Stenostomum sphagnetorum* (31). In each case, the secreted morphogen is proteinaceous. The factor released by the rotifer *Asplanchna brightwelli*

that induces spine development in the prey rotifer, *Brachionus calciflours*, also is a protein (32). In addition to releasing a morphogen that affects its prey, females of *A. brightwelli* are polymorphic in response to available food (33). This polymorphism is controlled by direct exposure of developing embryos to α-tocopherol in the diet of the mother (34), a substance that also induces the formation of a large oral apparatus in the protozoan *Blepharisma americanum* (35) and enhances differentiation in *T. vorax* (26). The predator/prey kairomone, which is released by the midge *Chaoborus americanus* and induces development of antipredator morphology in *Daphnia pulex*, resembles the inducer in stomatin in several ways (36, 37). The kairomone from *C. americanus* is a small (molecular mass <500 Da), water-soluble, heat-stable organic molecule, which is contained in clear, pale yellow fluid derived from the predator; however, unlike the inducer in stomatin, this morphogen binds to anion exchange resin and gives only one active fraction when separated by reversed-phase HPLC from water in which the predator has been grown. This kairomone has been identified as a nonolefinic hydroxyl-carboxylic acid.

The results of our study suggest that the signaling properties of environmental iron complexes may not be limited to regulating iron availability, but also may influence fundamental processes including development. Current efforts are directed toward elucidation of the chelated structure and identification of the mechanisms by which the complex is recognized and subsequently triggers differentiation.

We thank Marsha Donaldson for her technical assistance with the measurement of iron, and Drs. Margaret D. Johnson, John A. Boyle, and Kenneth O. Willeford for their critical reading of the manuscript.

1. Kühn, L. C. (1998) *Nutr. Rev.* **56,** S11–S19.
2. Radisky, D. & Kaplan, J. (1999) *J. Biol. Chem.* **274,** 4481–4484.
3. Theil, E. C. (1998) *Met. Ions Biol. Syst.* **35,** 403–434.
4. Baker, E., Baker, S. M. & Morgan, E. H. (1998) *Biochim. Biophys. Acta* **1380,** 21–30.
5. Oshiro, S., Nakamura, Y., Ishige, R., Hori, M., Nakajima, H. & Gahl, W. E. (1994) *J. Biochem.* **115,** 849–852.
6. Randell, E. W., Parkes, J. G., Olivieri, N. F. & Templeton, D. M. (1994) *J. Biol. Chem.* **269,** 16046–16053.
7. Trinder, D. & Morgan, E. (1998) *Am. J. Physiol.* **275,** G279–G286.
8. Smith, H. E. (1982) *J. Protozool.* **29,** 616–627.
9. Smith, H. E. (1982) *Trans. Am. Microsc. Soc.* **101,** 36–58.
10. Smith-Somerville, H. E., Verchot, M. E. & Ryals, P. E. (1986) *J. Protozool.* **33,** 261–266.
11. Buhse, H. E., Jr. (1967) *J. Protozool.* **14,** 608–613.
12. Butzel, H. M. & Fischer, J. (1983) *J. Protozool.* **30,** 247–250.
13. Grelland, E. M. (1988) *Eur. J. Protistol.* **24,** 52–59.
14. Ryals, P. E., Buhse, H. E., Jr. & Modzejewski, J. (1989) *Biochim. Biophys. Acta* **991,** 438–444.
15. Leboy, P. S., Cline, S. G. & Conner, R. L. (1964) *J. Protozool.* **11,** 217–222.
16. Buhse, H. E., Jr. (1966) *J. Protozool.* **13,** 429–435.
17. Nelsen, E. M., Frankel, J. & Martel, E. (1981) *Dev. Biol.* **88,** 27–38.
18. Thompson, G. A., Jr. (1967) *Biochemistry* **6,** 2015–2022.
19. Anderson, F. S. & Murphy, R. C. (1976) *J. Chromatogr.* **121,** 251–262.
20. Loefer, J. B., Owen, R. D. & Christensen, E. (1958) *J. Protozool.* **5,** 209–217.
21. Sherman, G. B., Buhse, H. E., Jr. & Smith, H. E. (1981) *Trans. Am. Microsc. Soc.* **100,** 366–372.
22. Smith, P. K., Krohn, R. I., Hermanson, G. T., Mallia, A. K., Gartner, F. H., Provenzano, M. D., Fujimoto, E. K., Goeke, N. M., Olson, B. J. & Klenk, D. C. (1985) *Anal. Biochem.* **150,** 76–85.
23. Bradford, M. M. (1976) *Anal. Biochem.* **72,** 248–254.
24. Albert, A. (1953) *Biochem. J.* **54,** 646–654.
25. Acevedo-Chávez, R., Costas, M. E. & Escudero, R. (1996) *Inorg. Chem.* **35,** 7430–7439.
26. Ryals, P. E. & Smith-Somerville, H. E. (1985) *Trans. Am. Microsc. Soc.* **104,** 341–349.
27. Martin, R. B. & Mariam, Y. H. (1979) in *Metal Ions in Biological Systems*, ed. Sigel, H. (Dekker, New York), Vol. 8, pp. 57–125.
28. Ryals, P. E., Bae, S. & Patterson, C. E. (1999) *J. Eukaryotic Microbiol.* **46,** 77–83.
29. Kusch, J. & Heckmann, K. (1992) *Dev. Genet.* **13,** 241–246.
30. Kusch, J. (1993) *Oecologia* **96,** 354–359.
31. Kusch, J. (1993) *J. Exp. Zool.* **265,** 613–618.
32. Gilbert, J. J. (1966) *Science* **151,** 1234–1237.
33. Gilbert, J. J. & Thompson, G. A., Jr. (1968) *Science* **159,** 734–738.
34. Birky, C. W., Jr. & Gilbert, J. J. (1972) *J. Embryol. Exp. Morphol.* **27,** 103–120.
35. Lennartz, D. C. & Bovee, E. C. (1980) *Trans. Am. Microsc. Soc.* **99,** 310–317.
36. Parejko, K. & Dodson, S. (1990) *Hydrobiologia* **198,** 51–59.
37. Tollrian, R. & von Elert, E. (1994) *Limnol. Oceanogr.* **39,** 788–796.
38. Stewart, G. W., Argent, A. C. & Dash, B. C. (1993) *Biochim. Biophys. Acta* **25,** 15–25.